

Primary Intermediates of Oxygen Photoevolution Reaction on TiO₂ (Rutile) Particles, Revealed by in Situ FTIR Absorption and Photoluminescence Measurements

Ryuhei Nakamura and Yoshihiro Nakato*

Contribution from the Division of Chemistry, Graduate School of Engineering Science, Osaka University, Toyonaka, Osaka 560-8531, Japan, and Core Research for Evolutional Science and Technology, Japan Science and Technology Agency (CREST, JST)

Received October 3, 2003; E-mail: nakato@chem.es.osaka-u.ac.jp

Abstract: Primary intermediates of oxygen photoevolution (water photooxidation) reaction at the TiO₂ (rutile)/aqueous solution interface were investigated by in situ multiple internal reflection infrared (MIRIR) absorption and photoluminescence (PL) measurements. UV irradiation of TiO₂ in the presence of 10 mM Fe³⁺ in the solution caused the appearance of a new peak at 838 cm⁻¹ and a shoulder at 812 cm⁻¹. Detailed investigations of the effects of solution pH, the presence of methanol as a hole scavenger, and isotope exchange in water (H₂¹⁶O→H₂¹⁸O) on the spectra have shown that the 838- and 812-cm⁻¹ bands can be assigned to the O–O stretching mode of surface TiOOH and TiOOTi, respectively, produced as primary intermediates of the oxygen photoevolution reaction. The results give strong support to our previously proposed mechanism that the oxygen photoevolution is initiated by a nucleophilic attack of a H₂O molecule on a photogenerated hole at a surface lattice O site, not by oxidation of surface OH group by the hole. The conclusion is supported by PL measurements. A plausible reaction scheme is proposed for the oxygen photoevolution on TiO₂ (rutile) in aqueous solutions of pH less than about 12.

Introduction

Photoinduced oxidation of water and organic compounds at TiO₂ or related metal-oxide semiconductor surfaces has attracted much attention from the points of view of solar-to-chemical conversion (water splitting)^{1–4} and environmental cleaning (photodecomposition of dirt or harmful materials).^{5–7} Recently, this reaction prompted new interest by the finding^{8–10} of a photo-induced increase in the hydrophilicity of the TiO₂ surface. In addition, this reaction has recently become more and more attractive by another finding^{11–19} that doping of metal oxides

such as TiO₂ with nitrogen, sulfur, carbon, or other elements leads to an extension of the photoactivity to the visible-light region.

For achieving successful applications of the phenomena to energy and environmental technologies, the improvement of the efficiency and stability through elucidation of reaction mechanisms is of essential importance. A number of studies have been made on the reaction mechanism of oxygen photoevolution on TiO₂ electrodes or particles, using electrochemical^{20–32} and spectroscopic^{33–47} methods, but reported mechanisms are rather scattered, and detailed mechanisms still remain unclear.

For example, Wilson et al. first reported²⁰ the formation of a surface state as a possible intermediate of oxygen photoevolution reaction on n-TiO₂, as detected by a negative potential sweep after UV irradiation under anodic bias. Salvador et al. studied the reaction mechanism in detail^{21–24} and reported that the Wilson's surface state could be attributed to adsorbed hydrogen

- (1) Fujishima, A.; Honda, K. *Nature* **1972**, *238*, 37.
- (2) Sato, S.; White, M. J. *Chem. Phys. Lett.* **1980**, *72*, 83.
- (3) Khan, S. U. M.; Al-Shahry, M.; Ingler, W. B., Jr. *Science* **2002**, *297*, 2243.
- (4) Kato, H.; Asakura, K.; Kudo, A. *J. Am. Chem. Soc.* **2003**, *125*, 3082.
- (5) Ollis, D. S.; Al-Ekabi, H., Eds. *Photocatalytic Purification and Treatment of Water and Air*; Elsevier: Amsterdam, 1993.
- (6) Fujishima, A.; Rao, T. N.; Tryk, D. A. *J. Photochem. Photobiol., C* **2000**, *1*, 1.
- (7) Hoffmann, M. R.; Martin, S. T.; Choi, W.; Bahnemann, D. W. *Chem. Rev.* **1995**, *95*, 69.
- (8) Wang, R.; Hashimoto, K.; Chikuni, M.; Kojima, E.; Kitamura, A.; Shimohigashi, M.; Watanabe, T. *Nature* **1997**, *388*, 431.
- (9) Sakai, N.; Fujishima, A.; Watanabe, T.; Hashimoto, K. *J. Phys. Chem. B* **2003**, *107*, 1028.
- (10) White, J. M.; Szanyi, J.; Henderson, M. A. *J. Phys. Chem. B* **2003**, *107*, 1028.
- (11) Kudo, A. *Catal. Surveys Asia* (online journal) **2003**, *7*, 31.
- (12) Sato, S. *Chem. Phys. Lett.* **1986**, *123*, 126.
- (13) Asahi, R.; Morikawa, T.; Ohwaki, T.; Aoki, K.; Taga, Y. *Science* **2001**, *293*, 269.
- (14) Hitoki, G.; Takata, T.; Kondo, J. N.; Hara, M.; Kobayashi, H.; Domen, K. *Chem. Commun.* **2002**, 1698.
- (15) Ishikawa, A.; Takata, T.; Kondo, J. N.; Hara, M.; Kobayashi, H.; Domen, K. *J. Am. Chem. Soc.* **2002**, *124*, 13547.
- (16) Kato, H.; Kudo, A. *J. Phys. Chem. B* **2002**, *106*, 5029.
- (17) Zou, A.; Ye, J.; Sayama, K.; Arakawa, H. *Nature* **2001**, *414*, 625.
- (18) Ohno, T.; Mitsui, T.; Matsumura, M. *Chem. Lett.* **2003**, *32*, 364.

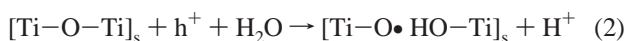
- (19) Irie, H.; Watanabe, Y.; Hashimoto, K. *Chem. Lett.* **2003**, *32*, 772.
- (20) Wilson, R. H. *J. Electrochem. Soc.* **1980**, *127*, 228.
- (21) Salvador, P.; Gutiérrez, C. *Chem. Phys. Lett.* **1982**, *86*, 131.
- (22) Salvador, P.; Gutiérrez, C. *J. Phys. Chem.* **1984**, *88*, 3696.
- (23) Salvador, P.; Gutiérrez, C. *J. Electroanal. Chem.* **1984**, *160*, 117.
- (24) Salvador, P.; Gutiérrez, C. *Surf. Sci.* **1983**, *124*, 398.
- (25) Nakato, Y.; Tsumura, A.; Tsubomura, H. *Chem. Phys. Lett.* **1982**, *85*, 387.
- (26) Nakato, Y.; Tsumura, A.; Tsubomura, H. *J. Phys. Chem.* **1983**, *87*, 2402.
- (27) Nakato, Y.; Ogawa, H.; Moria, K.; Tsubomura, H. *J. Phys. Chem.* **1986**, *86*, 6210.
- (28) Ulmann, M.; Tacconi, N. R.; Augustynski, J. *J. Phys. Chem.* **1986**, *90*, 6523.
- (29) Ulmann, M.; Augustynski, J. *Chem. Phys. Lett.* **1987**, *141*, 154.
- (30) Gerischer, H. *Electrochim. Acta* **1990**, *35*, 1677.
- (31) Smandex, B.; Gerischer, H. *Electrochim. Acta* **1989**, *34*, 1411.
- (32) Poznyak, K. S.; Sviridov, V. V.; Kulak, A. I.; Samstov, M. P. *J. Electroanal. Chem.* **1992**, *340*, 73.

peroxide, H₂O_{2 ad}, produced by coupling of surface •OH radicals formed through oxidation of surface OH group (Ti–OH_s) with photogenerated holes (h⁺)



Many other workers have also assumed reaction 1 as the initiation step of the oxygen photoevolution reaction on TiO₂.

On the other hand, we found^{25–27,48–52} that a photoluminescence (PL) band peaking at 840 nm was emitted from a UV-illuminated n-TiO₂ surface. Our later detailed studies^{51,52} using in situ photocurrent and PL measurements have shown that the PL band is emitted only from the (100) face of TiO₂ (rutile) and is assigned to an electronic transition from the conduction band to a vacant level of a “surface-trapped hole”, which acts as a precursor of the oxygen photoevolution reaction. Our studies have also shown that the oxygen photoevolution is not initiated by reaction 1 but by a nucleophilic attack of an H₂O molecule to a surface-trapped hole at a surface lattice O site accompanied by bond breaking.



The (100) face of TiO₂ (rutile) has the unique atomic structure, and thus the surface-trapped hole at this face is expected⁵¹ to lie at the bottom of atomic grooves present at this face (cf. Figure 9) and be stabilized by steric hindrance enough to emit a recombination luminescence as the PL, contrary to the case of other faces. It is worth noting here that reaction 1 is an electron-transfer-type reaction, whereas reaction 2 is a Lewis acid–base-type reaction, and therefore their energetics and kinetics are quite different from each other.

There is also confusion in mechanistic studies concerning spectroscopic methods. Jaeger and Bard⁵³ and recently Schwarz et al.⁵⁴ reported that by using a spin-trapping method hydroxyl (•OH) radicals were produced on UV-irradiated TiO₂ powder in aqueous solutions. However, it was pointed out by Nosaka

et al.⁵⁵ that the water photooxidation reaction at TiO₂ produced no free •OH radical and spin-trapping agents reacted with “surface-trapped holes” (assigned to adsorbed •OH radicals), giving ESR signals similar to those reported. The ESR detection of •OH radicals on irradiated TiO₂ (anatase) at 77 K was also reported by Anpo et al.,⁵⁶ although their ESR signals showed no spectral change by H₂O → D₂O exchange. On the other hand, Howe and Grätzel⁵⁷ first reported by ESR measurements that photogenerated holes were trapped at lattice O atoms (or Ti–O–Ti sites) at low temperatures of 4.2 or 77 K and did not produce •OH radicals. Later Micic et al.^{58,59} confirmed this conclusion and showed clearly that not •OH radicals but Ti–O• radicals were produced, in harmony with the mechanism of reaction 2.

The surface intermediates on irradiated TiO₂ were also studied by other spectroscopic methods. Szczepankiewicz et al.⁶⁰ reported by diffuse reflectance FTIR spectroscopy that a new band, assignable to surface •OH radicals, appeared at 3683 cm^{–1} for UV-irradiated TiO₂ (P25 and pure anatase) powder in an oxygen atmosphere. Yates et al.,⁶¹ on the other hand, reported that •OH radicals did not play any important role in photoinduced oxidation of trichloroethylene on TiO₂ (P25) in the gas phase. Hashimoto et al.⁶² also reported, by measuring the quantum yield of formation of •OH radicals by means of a fluorescence probe method, that the formation of •OH radicals was not the major process on irradiated TiO₂ (anatase) in aqueous solutions. In addition, recent ultraviolet photoelectron spectroscopic (UPS) studies,^{63–65} combined with scanning tunnel microscopic (STM) inspection,^{63,66} revealed that the O-2p levels for bridging hydroxyl groups (Ti–OH–Ti) at the (110) face and terminal hydroxyl groups (Ti–OH) at the (100) face are both far below the top of the valence band of TiO₂ (rutile).

It is evident that in situ direct spectroscopic detection of reaction intermediates is of crucial importance for clarification of molecular mechanisms. Very recently, we reported⁶⁷ that multiple internal reflection (MIR) infrared (IR) absorption spectroscopy could be successfully applied to in situ observation of primary intermediates of photocatalytic O₂ reduction on TiO₂ in contact with aqueous solutions. The IR spectroscopy has, in general, a serious difficulty in application to aqueous systems owing to strong IR absorption of water.⁶⁸ The difficulty can be overcome to a large extent by using internal reflection techniques.⁶⁹ The single internal reflection (SIR) mode was suc-

- (33) Lawless, D.; Serpone, N.; Meisel, D. *J. Phys. Chem.* **1990**, *94*, 331.
 (34) Rajh, T.; Sapomjic, Z. V.; Micic, O. I. *Langmuir* **1992**, *8*, 1265.
 (35) Nakaoka, Y.; Nosaka, Y. *J. Photochem. Photobiol., A* **1997**, *110*, 299.
 (36) Liao, L.-F.; Lien, C.-F.; Shieh, D.-L.; Chen, M.-T.; Lin J.-L. *J. Phys. Chem. B* **2002**, *106*, 11240.
 (37) Szczepankiewicz, S. H.; Moss, J. A.; Hoffmann, M. R. *J. Phys. Chem. B* **2002**, *106*, 7654.
 (38) Christensen, P. A.; Eameaim, J.; Hamnett, A.; Lin, W. F. *Chem. Phys. Lett.* **2001**, *344*, 488.
 (39) Fujihara, K.; Izumi, S.; Ohno, T.; Matsumura, M. *J. Photochem. Photobiol. A* **2000**, *132*, 99.
 (40) Ikeda, S.; Sugiyama, N.; Pal, B.; Marcić, G.; Palmisano, L.; Noguchi, H.; Uosaki, K.; Ohtani, B. *Phys. Chem. Chem. Phys.* **2001**, *3*, 267.
 (41) Shaw, K.; Christensen, P.; Hamnett, A. *Electrochim. Acta* **1996**, *41*, 710.
 (42) Yamakata, A.; Ishibashi, T.; Onishi, H. *J. Mol. Catal. A: Chem.* **2003**, *199*, 85.
 (43) Yamakata, A.; Ishibashi, T.; Onishi, H. *J. Phys. Chem. B* **2003**, *107*, 9820.
 (44) Wang, C.-y.; Groenzin, H.; Sultz, M. *J. Langmuir* **2003**, *19*, 7330.
 (45) Nakamura, R.; Sato, S. *Langmuir* **2002**, *18*, 4433.
 (46) Nakamura, R.; Sato, S. *J. Phys. Chem. B* **2002**, *106*, 5893.
 (47) Diebold, U. *Surf. Sci. Rep.* **2003**, *48*, 53.
 (48) Nakato, Y.; Akanuma, H.; Shimizu, J.-I.; Magari, Y. *J. Electroanal. Chem.* **1995**, *396*, 35.
 (49) Magari, Y.; Ochi, H.; Yae, S.; Nakato, Y. *Solid/Liquid Electrochemical Interfaces*; ACS Symposium Series 656; The American Chemical Society: Washington, DC, 1996; p 297.
 (50) Nakato, Y.; Akanuma, H.; Magari, Y.; Yae, S.; Shimizu, J.-I.; Mori, H. *J. Phys. Chem. B* **1997**, *101*, 4934.
 (51) Kisumi, T.; Tsujiko, A.; Murakoshi, K.; Nakato, Y. *J. Electroanal. Chem.* **2003**, *545*, 99.
 (52) Tsujiko, A.; Kisumi, T.; Magari, Y.; Murakoshi, K.; Nakato, Y. *J. Phys. Chem. B* **2000**, *104*, 4873.
 (53) Jaeger, C. D.; Bard, A. J. *J. Phys. Chem.* **1979**, *83*, 3146.
 (54) Schwarz, P. F.; Turro, N. J.; Bossmann, S. H.; Braun, A. M.; Wahab, A.-M. A.; Dürr, H. *J. Phys. Chem. B* **1997**, *101*, 7127.

- (55) Nosaka, Y.; Komori, S.; Yawata, K.; Hirakawa, T.; Nosaka, Y. A. *Phys. Chem. Chem. Phys.* **2003**, *5*, 4731.
 (56) Anpo, M.; Shima, T.; Kubokawa, Y. *Chem. Lett.* **1985**, 1799.
 (57) Howe, R. F.; Grätzel, M. *J. Phys. Chem.* **1987**, *91*, 3906.
 (58) Micic, O. I.; Zhang, Y.; Cromack, K. R.; Trifunac, A. D.; Thurnauer, M. C. *J. Phys. Chem.* **1993**, *97*, 7277.
 (59) Micic, O. I.; Zhang, Y.; Cromack, K. R.; Trifunac, A. D.; Thurnauer, M. C. *J. Phys. Chem.* **1993**, *97*, 13284.
 (60) Szczepankiewicz, S. H.; A. Colussi, J.; Hoffmann, M. R. *J. Phys. Chem. B* **2000**, *104*, 9842.
 (61) Fan, J.; Yates, J. T., Jr. *J. Am. Chem. Soc.* **1996**, *118*, 4686.
 (62) Ishibashi, K.; Fujishima, A.; Watanabe, T.; Hashimoto, K. *J. Photochem. Photobiol., A* **2000**, *134*, 139.
 (63) Brookes, I. M.; Muryn, C. A.; Thornton, G. *Phys. Rev. Lett.* **2001**, *87*, 266103.
 (64) Muryn, C. A.; Hardman, P. J.; Crouch, J. J.; Raiker, G. N.; Thornton, G. D.; Law, S. L. *Surf. Sci.* **1991**, *215–242*, 747.
 (65) Henderson, M. A. *Surf. Sci. Rep.* **2002**, *46*, 1.
 (66) Schaub, R.; Thosttrup, P.; Lopez, N.; Lægsgaard, E.; Stensgaard, I.; Nørskov, J. K.; Besenbacher, F. *Phys. Rev. Lett.* **2001**, *87*, 266104.
 (67) Nakamura, R.; Imanishi, A.; Murakoshi, K.; Nakato, Y. *J. Am. Chem. Soc.* **2003**, *125*, 7443.
 (68) Clark, R. J. H.; Hester, R. E. *Spectroscopy for Surface*; John Wiley & Sons: New York, 1998; p 219–272.
 (69) Sućetka, W. *Surface Infrared and Raman Spectroscopy*; Plenum Press, New York, 1996.

cessfully applied to detection of various interfacial species by McQuillan et al.^{70–74} The advantage of the MIR mode lies in its high detection sensitivity. This mode can detect a surface species of a submonolayer amount even in contact with an aqueous medium.

In the present work, we have applied the MIR-IR technique to detection of surface intermediates of the oxygen photoevolution reaction on particulate TiO₂ (rutile) films. A diamond single-crystal prism was used as an internal reflection element (IRE), instead of a ZnSe prism in a previous work,⁶⁷ to get high spectral sensitivity in a low-frequency region from 1500 to 600 cm⁻¹ in which surface intermediates of the oxygen photoevolution reaction are expected to show vibrational bands. We have succeeded in detecting surface peroxo species as primary intermediates of the oxygen photoevolution reaction, which supports reaction 2 as the initiation reaction.

Experimental Section

TiO₂ powder, called JRC-TIO-3 by the Catalysis Society of Japan, was used for the multiple internal reflection infrared (MIR-IR) measurements. The powder is well characterized by the Society as one of the reference catalysts and is reported to be composed of 100% rutile particles with the average primary diameter (d_{av}) of 30–50 nm and surface area of 51 m²/g. The surface of the TiO₂ particles was first cleaned by heating at 600 °C in an O₂ atmosphere for 5 h, followed by UV-irradiation in O₂-saturated water for 1 h and ultrasonic agitation for 30 min. The cleaned particles were then dried and kept under vacuum ($<1 \times 10^{-3}$ Torr).

Single-crystal TiO₂ (rutile) wafers for PL measurements were obtained from Earth Chemical Co., Ltd. They had 99.99% in purity, 10 mm × 10 mm in area and 1.0 mm in thickness, and (110)-cut alkali-polished surfaces. The wafers were washed by rinsing with acetone and ultrasonic agitation in pure water for 5 min, and reduced in a stream of hydrogen at 550 °C for 3 h to get n-type semiconductivity. Specimens of about 0.3 Ω cm were used for experiments.

All other chemicals, H₂¹⁸O (Aldrich, 99.9 at. %), NaOH (Wako), HCl (Wako), H₂SO₄ (Wako), Na₂SO₄ (Wako), H₂O₂ (Wako), methanol (Wako), and FeCl₃ (Aldrich), were of reagent grade and used as received without further purification. Solutions were prepared using pure (Milli-Q) water with a conductivity of 18 MΩ¹⁻ cm⁻¹. Nitrogen or oxygen gas was bubbled through the solution either to remove dissolved air (oxygen) or to dissolve oxygen.

A spectral cell for the MIR-IR experiment is illustrated schematically in Figure 1. A diamond single-crystal disk of 3 mm in diameter and 0.25 mm in thickness, affixed to a ZnSe single crystal having an inlet and an outlet for IR light was used as the internal reflection element (IRE). An experimental set (for MIR experiments) furnished with this IRE and reflection mirrors was commercially available, and we obtained it from S. T. Japan Inc. In most cases, 10 μL of aqueous TiO₂ slurry (10 mg/mL) was spread on the diamond disk with a plastic pipet and dried in air. The inner volume of the cell, including the aqueous solution, was approximately 40 μL. The IR light was reflected about 9 times at the diamond/TiO₂ solution interface, as calculated from the geometry of the IRE.

The spectral cell was placed in the sample chamber of an FTIR spectrometer (Bio-Rad FTS 575C) with a deuterated triglycine sulfate (DTGS) detector. Before measurements, the sample chamber was purged with N₂ and the TiO₂ film was kept in the dark for about 60 min. The IR intensity (I) vs wavelength (λ) was obtained by averaging

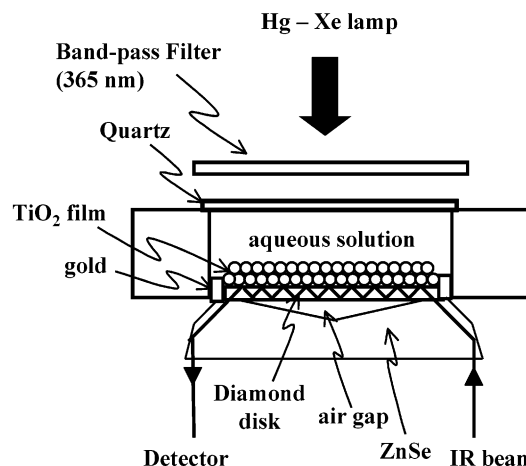


Figure 1. Schematic illustration of a spectral cell used for in situ MIR-IR absorption measurements.

400 scans at a resolution of 4 cm⁻¹, with a processing time of 6 min for one spectrum. All MIRIR absorption spectra were obtained in the form of absorbance, $\log(I_0/I)$, using an appropriate reference sample giving I_0 .

UV irradiation of the TiO₂ film was carried out by a 365-nm band from a 200-W Hg–Xe lamp (Hypercure 200 UV, Yamashita Denso) with an optical guide, chosen by use of a band-pass filter (Asahi Techno Glass UV-D36A). A neutral density (metal net) filter and an IR-cut filter were also used to avoid cell heating. The incident UV light intensity at the position of the sample surface was approximately 1 mW cm⁻², as measured with a thermopile (Eppley Laboratory). Further details on the MIRIR method were described in a previous paper.⁶⁷

Photocurrent density (j) vs potential (U) curves for single-crystal n-TiO₂ electrodes were measured with a commercial potentiostat and a potential programmer, using a Pt plate as the counter electrode and an “Ag/AgCl/sat. KCl” electrode as the reference electrode. The illumination was carried out by the 365-nm band from a 500-W high-pressure mercury lamp, obtained by use of band-pass filters. The PL intensity (I_{PL}) vs U curves were measured simultaneously with the j – U curve measurements.

Results

In Situ FTIR Measurements. Figure 2 shows MIR-IR absorption spectra for a particulate TiO₂ film in contact with a deoxygenated aqueous solution of 10 mM Fe³⁺ (pH 2.4). The absorption spectra after UV irradiation are plotted as a function of the illumination time, with the TiO₂ film before UV irradiation taken as the spectral reference. In general, both photogenerated conduction-band electrons (e⁻) and valence-band holes (h⁺) cause photoreactions at the TiO₂ surface for a particulate system, each producing various surface intermediates. The Fe³⁺ ions in Figure 2 were added to the solution as an electron scavenger to suppress the formation of surface intermediates caused by the conduction-band electrons.⁶⁷

The UV irradiation caused the appearance of a new peak at 838 cm⁻¹ and shoulders at 812 and 928 cm⁻¹, as seen in Figure 2. The shoulder at 812 cm⁻¹ was relatively prominent in the short irradiation times of 1 and 10 min, contrary to the 928-cm⁻¹ band. The noise level in the region from 700 to 1000 cm⁻¹ was confirmed to be less than 2×10^{-4} in absorbance after averaging by 400-time accumulation adopted in the present work. The appearance of the new bands at 838 and 812 cm⁻¹ was independent of the presence or absence of dissolved oxygen in the solution, strongly suggesting that these bands were arising

(70) Connor, P. A.; McQuillan, A. J. *Langmuir* **1999**, *15*, 2916.

(71) Ronson, T. K.; McQuillan, A. J. *Langmuir* **2002**, *18*, 5019.

(72) Nazeeruddin, M. K.; Amiras, M.; Comte, P.; Mackay J. R.; McQuillan, A. J.; Houriet, R.; Grätzel, M. *Langmuir* **2000**, *16*, 8525.

(73) Connor, P. A.; Dobson, K. D.; McQuillan, A. J. *Langmuir* **1999**, *15*, 2402.

(74) Ekström, G. N.; McQuillan, A. J. *J. Phys. Chem. B* **1999**, *103*, 10562.

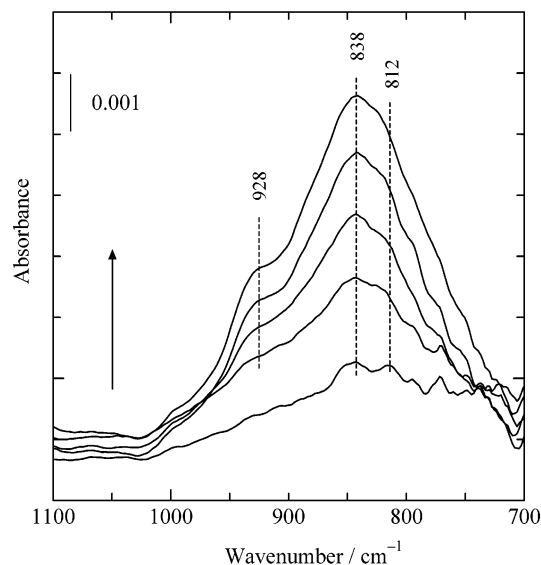


Figure 2. MIR-IR spectra of a TiO₂ film in contact with a deoxygenated aqueous solution of 10 mM Fe³⁺ (pH 2.4), recorded in 1, 10, 20, 30, and 40 min after the start of UV irradiation. A TiO₂ film before irradiation is taken as the reference. The arrow in the figure indicates the direction of the spectral change with the irradiation time.

from intermediates of oxidation reaction of water by photogenerated holes. The independence of the IR bands on the concentration of dissolved O₂ also indicates that the concentration of 10 mM Fe³⁺ is sufficiently high to capture all photogenerated electrons in TiO₂. In accordance with this result, Ohno et al. reported⁷⁵ that the quantum efficiency of the oxygen photoevolution for suspended TiO₂ in aqueous Fe³⁺ was independent of the Fe³⁺ concentration in the range of 2–8 mM Fe³⁺.

The diamond prism is completely transparent in a low-frequency region from 1500 to 600 cm⁻¹ and thus has a high spectral sensitivity in this region, as mentioned earlier. However, the prism has strong absorption in a region from 1900 to 2200 cm⁻¹, in which no spectral measurement is possible. Besides, the diamond prism shows a large number of absorption bands in a high-frequency region from 2300 to 4000 cm⁻¹ probably owing to impurities in crystal, and therefore the prism is not necessarily suitable for spectral measurements even in this high-frequency region. Nevertheless, in the present work, we could observe small decreases in absorption bands due to contaminating hydrocarbons at around 2900 cm⁻¹ by UV irradiation.

Spectra (a) in Figure 3 (solid lines) show FTIR spectra for a TiO₂ film in contact with a deoxygenated alkaline solution of pH 11.9, obtained by similar experiments to Figure 2. In this case, however, no electron scavenger was added to the solution because Fe³⁺ ions were unstable in pH ≥ 3, causing an oxyhydroxide precipitate. Instead we used Pt-loaded TiO₂ particles in which Pt could act as a kind of electron scavenger because hydrogen evolution occurred on Pt by the conduction-band electrons. Only the 812-cm⁻¹ band appeared by UV irradiation in an alkaline solution [spectra (a) in Figure 3], contrary to the case of an acidic solution in Figure 2. This result was confirmed by the fact that an FTIR spectrum [spectrum (b) in Figure 3] for Pt-loaded TiO₂, prepared in the same way as above, in contact with a deoxygenated acidic solution of pH

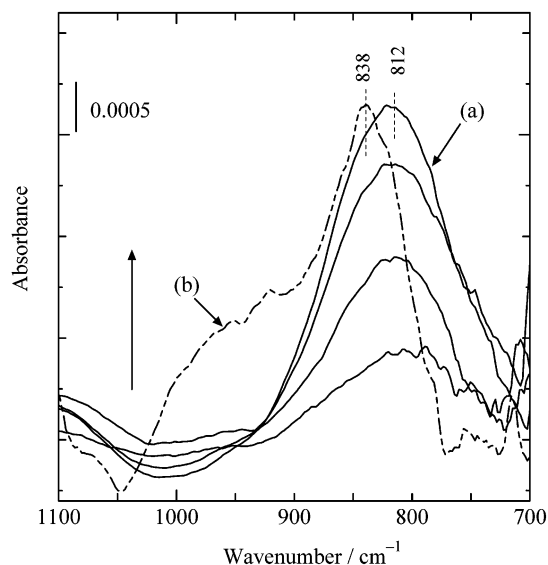


Figure 3. Spectra (a) (solid curves): MIR-IR spectra of a film of Pt-loaded TiO₂ in contact with aqueous 0.01 M NaOH of pH 11.9, recorded in 1, 20, and 30 min after the start of UV irradiation. The arrow in the figure indicates the direction of the spectral change with time. Spectrum (b) (broken curve): MIR-IR spectrum for Pt-loaded TiO₂ in contact with 0.01 M HCl of pH 2.4 after 30-min UV irradiation. Spectrum (b) is expanded by a factor of 1.4 in absorbance.

2.4 with no Fe³⁺, showed the main band at 838 cm⁻¹ and shoulders at 812 and 900–1000 cm⁻¹, similar to the spectra in Figure 2, although the bandwidth or shape is somewhat different between spectra in Figure 2 and spectrum (b) in Figure 3. The reason for such a difference in detailed spectral features is unknown at present. The appearance of the 812-cm⁻¹ band by UV irradiation in spectra (a) of Figure 3 is accompanied by a slight decrease in absorbance at about 1010 cm⁻¹, the reason for which is also unknown. Such small spectral deviations might most probably arise from low signal-to-noise ratios due to weak absorption intensities for the Pt-loaded TiO₂ system, owing to inefficient capture of conduction-band electrons by loaded Pt relative to Fe³⁺ ions.

We suggested above that the new bands at 838 and 812 cm⁻¹ were arising from intermediates of the hole-induced oxidation reaction of water. To confirm this conclusion, we did several experiments. First, we examined the effect of adding methanol as a hole scavenger to the solution. Figure 4A shows an MIRIR spectrum, before UV irradiation, for a TiO₂ film in contact with an aqueous solution of 10 mM Fe³⁺ containing 25 wt % methanol, the TiO₂ film in contact with an aqueous solution of 10 mM Fe³⁺ being taken as the spectral reference. The spectrum in Figure 4A shows bands at 1110, 1020, 944, and 905 cm⁻¹, of which the 1020- and 1110-cm⁻¹ bands can be assigned to the C–O stretching of methanol and methoxy (Ti–OCH₃) species, respectively.^{43,76} The origins of the 944- and 905-cm⁻¹ bands are at present unknown, although these bands are only observed for methanol-containing systems and evidently arise from methanol. The UV irradiation caused decreases in the intensities of these bands, as shown in Figure 4B, indicating the effective occurrence of photooxidation of methanol at the TiO₂ surface. (Note that the absorbance scale is different between A and B of Figure 4.) However, no absorption band appeared at 838 cm⁻¹ in Figure 4B, indicating no occurrence

(75) Ohno, T.; Haga, D.; Fujihara, K.; Kaizaki, K.; Matsumura, M. *J. Phys. Chem. B* **1997**, *101*, 6415.

(76) Yamakata, A.; Ishibashi, T.; Onishi, H.; *J. Phys. Chem. B* **2002**, *106*, 9122.

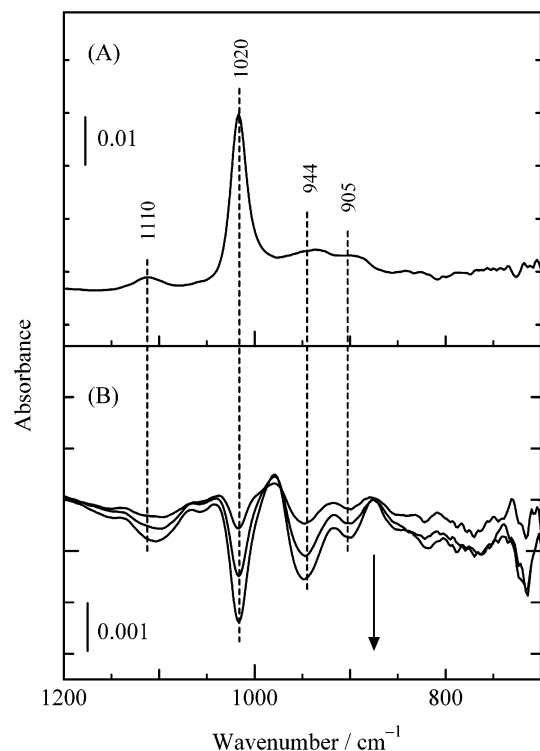


Figure 4. (A) MIR-IR spectrum before UV irradiation for a TiO₂ film in contact with an aqueous solution containing 10 mM Fe³⁺ and 25 wt % methanol. (B) MIR-IR spectra for the TiO₂ film, recorded in 1, 10, and 20 min after the start of UV irradiation. The arrow in the figure indicates the direction of the spectral change with time.

of the photooxidation of water. This result is quite reasonable if we take into account that methanol is more easily oxidized than water, and thus the oxidation of methanol suppresses the water oxidation.^{29,43,49} In other words, this result indicates that the band at 838 cm⁻¹ in Figure 2 is arising from intermediates of the photooxidation reaction of water. Similarly, no appearance of the 812-cm⁻¹ band was observed for Pt-loaded TiO₂ particles in an alkaline solution of pH 12.1 when 25 wt % methanol was added to the solution.

Second, we did isotope-labeling experiments by using H₂¹⁸O as a solvent. Spectrum (a) of Figure 5A shows the MIRIR spectrum for a particulate TiO₂ film in contact with H₂¹⁸O containing 10 mM Fe³⁺. Spectrum (b) is measured under the same conditions as (a) except that H₂¹⁶O is used. Spectrum (b) is thus the same as that in Figure 2. Both spectra (a) and (b) are monitored for a relatively short irradiation time of 20 min, because the shoulder bands are more prominently observed in the shorter irradiation time, as mentioned earlier. We can see that spectrum (a) is shifted to the lower frequency side than spectrum (b) and has a larger number of shoulders than spectrum (b). This result is also in harmony with the conclusion that the observed bands are arising from intermediates of the water photooxidation reaction, as discussed in detail in the next section. Figure 5B shows some spectra for TiO₂ in contact with H₂¹⁸O with 10 mM Fe³⁺, obtained independently by repeated experiments under the same conditions, to indicate the extent of experimental reproducibility in the spectra.

Third, we measured an MIR-IR spectrum for a particulate TiO₂ film on which hydrogen peroxide (H₂O₂) was adsorbed. Spectrum (a) in Figure 6 shows an IR spectrum for a particulate

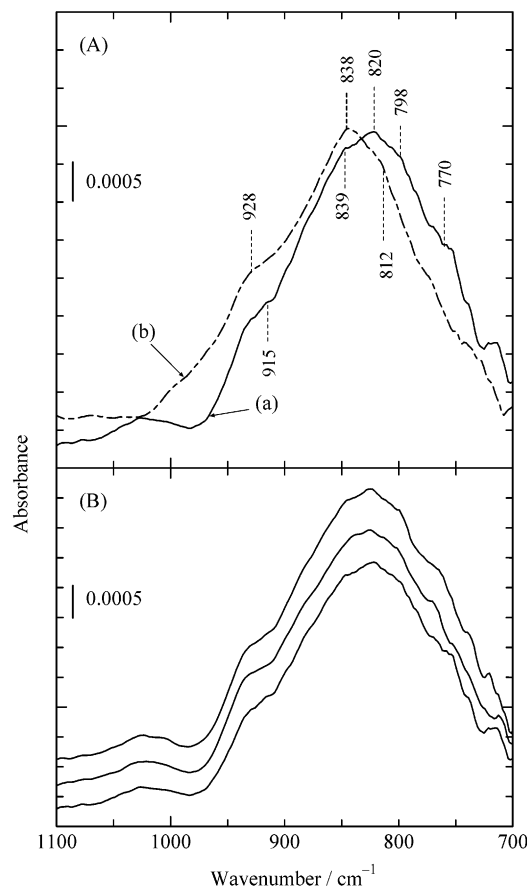


Figure 5. (A) MIR-IR spectra for a TiO₂ film in contact with (a) H₂¹⁸O and (b) H₂¹⁶O, both containing 10 mM Fe³⁺, observed after 20-min UV irradiation. (B) Spectra obtained independently by repeated experiments under the same conditions as for (a) of Figure 5A.

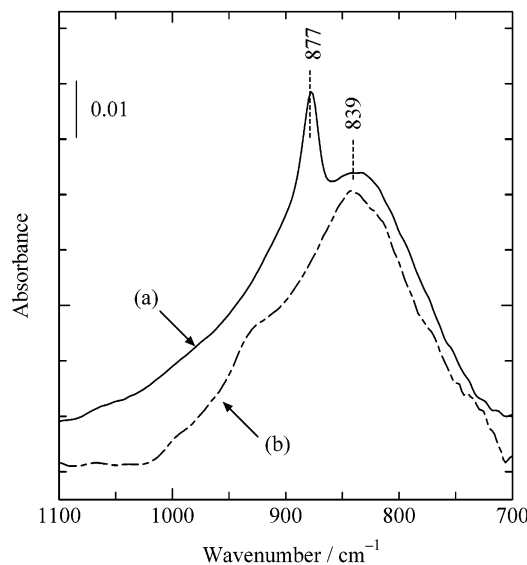


Figure 6. (a): MIR-IR spectrum of a TiO₂ film in contact with an aqueous solution of 30% H₂O₂. (b): Spectrum identical to that after the 20-min irradiation in Figure 2, for reference, with 13-times expansion in absorbance.

TiO₂ film exposed to an aqueous solution (pH 3.3) of 30% H₂O₂, with the TiO₂ film exposed to pure water used as the spectral reference. Spectrum (b) shows, for reference, the same spectrum as that in Figure 2 after the 20-min irradiation. We can see that

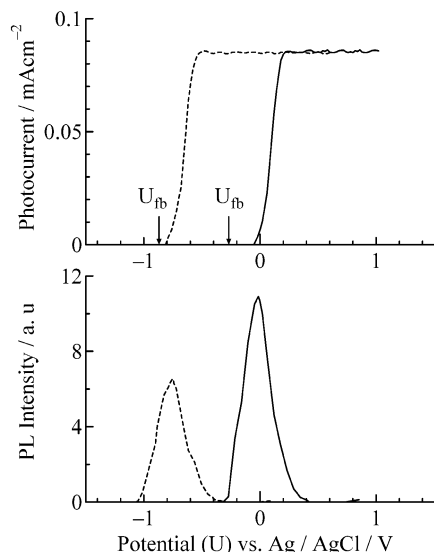


Figure 7. j - U and I_{PL} - U curves in an acidic (pH 1.2, solid curves) and an alkaline (pH 11.9, broken curves) solution for a photoetched n-TiO₂ electrode, observed by UV illumination at an intensity of 0.2 mW cm⁻². The I_{PL} is measured at 840 nm. The scan rate is 50 mV s⁻¹.

the exposure of TiO₂ to H₂O₂ gives rise to a band peaked at 839 cm⁻¹, which is nearly identical with the 838-cm⁻¹ band in Figure 2, and an additional sharp band at 877 cm⁻¹. The latter 877-cm⁻¹ band was observed when a diamond prism (IRE) with no TiO₂ film was exposed to the H₂O₂ solution, indicating that it can be assigned to free (or physically adsorbed) H₂O₂.^{77,78} On the other hand, the former 839-cm⁻¹ band was observed only for a diamond prism with a TiO₂ film.

In Situ PL Measurements. We reported in previous papers^{25-27,48-52} that photoelectrochemical etching of single-crystal n-TiO₂ (rutile) electrodes in aqueous H₂SO₄ produced rectangular nanoholes or grooves in the <001> direction, with the (100) face selectively exposed at the walls of the holes and grooves. We also reported that the PL band peak at 840 nm was observed only for the photoetched and thus the (100)-face exposed electrodes.^{51,52} Figure 7 shows the photocurrent (j) vs potential (U) and the PL intensity (I_{PL}) vs U for such a photoetched n-TiO₂ (rutile) electrode in an acidic (pH 1.2) and an alkaline (pH 11.9) solution. The UV irradiation was performed at 0.2 mW cm⁻². Both the I_{PL} vs U and the j vs U curves were measured in a positive potential scan simultaneously. The reported flat-band potential (U_{fb}) for rutile n-TiO₂^{79,80} is indicated with a pH-correction of 0.059 V/pH. The PL intensity takes the maximum near the onset potential of the photocurrent, indicating that this is a surface carrier recombination luminescence. The weakening of the PL in potentials more negative than the U_{fb} can be explained to be due to chemical reduction of the TiO₂ surface (or formation of some reduced surface species such as Ti³⁺ acting as nonradiative recombination centers).

Figure 8 shows PL spectra for a photoetched n-TiO₂ (rutile) electrode. Spectrum (a) was observed in an acidic (pH 1.2) solution at 0 V vs Ag/AgCl, whereas spectrum (b) was ob-

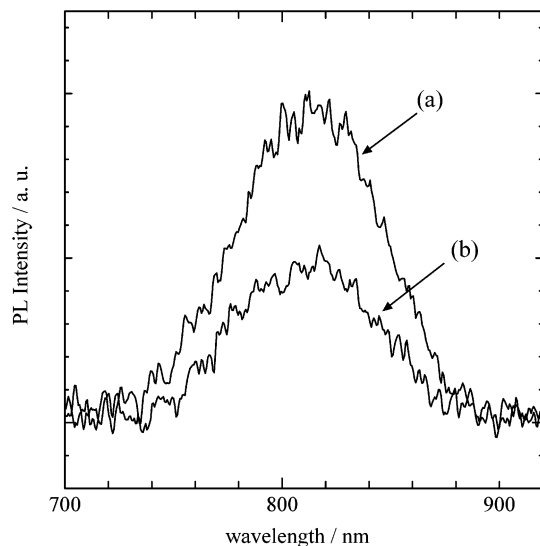


Figure 8. PL spectrum for a photoetched n-TiO₂ electrode, observed in (a) acidic (pH 1.2) and (b) alkaline (pH 12.8) solutions.

served in an alkaline (pH 12.8) solution at -0.8 V, both with the irradiation intensity of 0.2 mW cm⁻². The spectral distributions of stray light, observed at 1.0 and 0.4 V, were taken as the background for spectra (a) and (b), respectively. The spectral shape of both spectra (a) and (b) was not corrected for the spectral sensitivity of a photomultiplier used (Hamamatsu Photonics PMA100), but we can see that the PL spectra in acidic and alkaline solutions had the same position and shape with each other, indicating that the PL-emitting species is free from an acid-base equilibrium (or protonation and deprotonation).

Discussion

We mentioned in the preceding section that the UV irradiation of a particulate TiO₂ film in contact with an acidic solution with 10 mM Fe³⁺ caused the appearance of new bands at 838, 812, and 928 cm⁻¹ (Figure 2). We also mentioned there that the new IR bands could be explained to be arising from surface intermediates of the oxygen photoevolution reaction on TiO₂ particles.

To what surface species are these bands assigned? The 838-cm⁻¹ band for UV-irradiated TiO₂ in Figure 2 can be assigned to the O-O stretching mode of surface TiOOH species for the following reasons. We have to note first in Figure 6 that this band is nearly identical with the 839-cm⁻¹ band for H₂O₂-adsorbed TiO₂ in their spectral position and shape. Recent IR studies reported⁷⁷ that the exposure of Ti-silicalite molecular sieves (TS-1) to 30% H₂O₂ gave two IR bands at 837 and 877 cm⁻¹ and that the former 837-cm⁻¹ band could be assigned to the O-O stretching mode of a surface hydroperoxo species (TiOOH), whereas the latter 877-cm⁻¹ band assigned to free H₂O₂. The IR bands at 839 and 877 cm⁻¹ in spectrum (a) of Figure 6 are quite the same as the reported bands at 837 and 877 cm⁻¹⁷⁷ and thus can be assigned in the same way as the literature.⁷⁷ This implies that the 838-cm⁻¹ band is assigned to TiOOH.

The shoulder at 812 cm⁻¹ in Figure 2, on the other hand, appears as the main peak in an alkaline solution [spectrum (a) of Figure 3]. This result can be understood reasonably if we assume that the 812-cm⁻¹ band is assigned to a surface peroxo

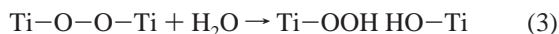
(77) Lin, W.; Frei, H. *J. Am. Chem. Soc.* **2002**, *124*, 9293.

(78) Tozzola, G.; Mantegazza, M. A.; Ranghino, G.; Petrini, G.; Bordiga, S.; Ricchiardi, G.; Lamberti, C.; Zullian, R.; Zecchina, A. *J. Catal.* **1998**, *179*, 64.

(79) Butler, M.; Ginley, D. D. *J. Electrochem. Soc.* **1979**, *125*, 228.

(80) Tomkiewicz, M. *J. Electrochem. Soc.* **1979**, *126*, 1505.

species of a bridge type, Ti–O–O–Ti. It is very likely that the oxygen photoevolution reaction first produces Ti–O–O–Ti as a surface intermediate, but in an acidic solution, it changes into a hydroperoxo species, Ti–OOH, by protonation (or acid-catalyzed hydrolysis).



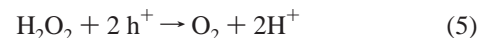
The assignment of the 812-cm⁻¹ band to Ti–O–O–Ti is also supported by IR studies of metal–dioxygen complexes,^{81–85} which report that the O–O stretching mode of a bridged peroxo species (*μ*-peroxo) is observed in a region of 790–840 cm⁻¹. A shoulder at 928 cm⁻¹ in Figure 2 may tentatively be assigned to the O–O stretching of surface peroxo species, Ti(O₂),^{67,86–89} produced by photocatalytic reduction of O₂ molecules evolved by the oxygen photoevolution reaction.

The above assignments for the 838- and 812-cm⁻¹ bands are in harmony with isotope-labeling experiments. Spectrum (a) in Figure 5A, observed for UV-irradiated TiO₂ in contact with H₂¹⁸O, shows a number of IR bands at 915, 839, 820, 798, and 770 cm⁻¹, which can be understood reasonably on the basis of the above assignments. It is reported,⁷⁷ by experiments of exposure of TS-1 to H¹⁸O¹⁸OH, that the O–O stretching band for TiOOH shifts from 837 cm⁻¹ for Ti–¹⁶O–¹⁶OH to 793 cm⁻¹ for Ti–¹⁸O–¹⁸OH, with an isotopic shift of 44 cm⁻¹. Accordingly we can assign the shoulder at 839 cm⁻¹ in spectrum (a) to the O–O stretching mode for Ti–¹⁶O–¹⁶OH, the peak at 820 cm⁻¹ to that for Ti–¹⁶O–¹⁸OH and Ti–¹⁸O–¹⁶OH, and the shoulder at 798 cm⁻¹ to that for Ti–¹⁸O–¹⁸OH. It is quite reasonable that an observed isotopic shift of 19 cm⁻¹ between Ti–¹⁶O–¹⁸OH or Ti–¹⁸O–¹⁶OH (820 cm⁻¹) and Ti–¹⁶O–¹⁶OH (838 cm⁻¹) is half the shift between Ti–¹⁶O–¹⁶OH (839 cm⁻¹) and Ti–¹⁸O–¹⁸OH (798 cm⁻¹).^{81–85} On the other hand, the shoulder at 770 cm⁻¹ can be assigned to the O–O stretching of Ti–¹⁸O–¹⁸O–Ti. The assignment also gives a reasonable isotope shift of 42 cm⁻¹ for Ti–¹⁶O–¹⁶O–Ti (812 cm⁻¹) and Ti–¹⁸O–¹⁸O–Ti (770 cm⁻¹).^{85–89}

On the basis of the above assignments, let us now consider the mechanism of the oxygen photoevolution reaction on TiO₂ (rutile). As mentioned in the Introduction section, we can say that two essentially different mechanisms have been proposed thus far. One mechanism assumes that the oxygen photoevolution is initiated by reaction 1, i.e., the oxidation of a surface OH group by a photogenerated hole, which can be called “surface-OH oxidation mechanism”. The other mechanism assumes that the water photooxidation is initiated by reaction 2, a nucleophilic attack of a H₂O molecule on a surface-trapped hole at a lattice O site, which can be called “nucleophilic attack mechanism”. In the former “surface-OH oxidation mechanism”, resultant surface •OH radicals, formed by reaction 1, couple with each other and produce H₂O₂.

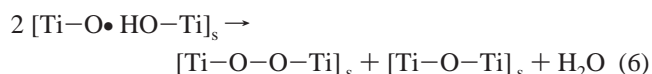


Resulting H₂O₂ is an easily oxidized compound, and it will be oxidized further by photogenerated holes, finally resulting in molecular oxygen.

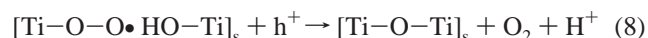
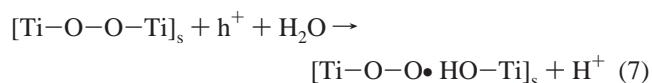


Accordingly, in the “surface-OH oxidation mechanism”, we can expect •OH_s, H₂O_{2 ad}, and Ti–OOH formed from H₂O_{2 ad}, as surface reaction intermediates.

On the other hand, in the “nucleophilic attack mechanism”, reaction 2 produces surface [Ti–O• HO–Ti]_s radicals accompanied by bond breaking. When two radicals [Ti–O• HO–Ti]_s are produced accidentally in adjacent positions, they couple with each other, forming surface peroxo species, TiOOTi.



Resultant [Ti–O–O–Ti]_s is expected to have a considerable steric distortion and thus be more reactive than the original [Ti–O–Ti]_s, and therefore it will easily cause a reaction similar to reaction 2, finally leading to oxygen evolution together with restoration of the original [Ti–O–Ti]_s.



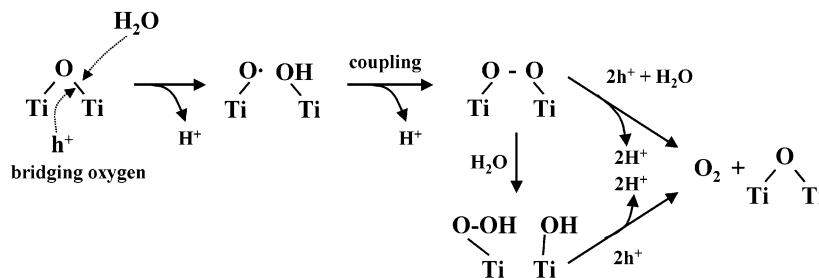
Thus, in this mechanism, we can expect [Ti–O–O–Ti]_s and Ti–OOH as surface intermediates.

The in situ FTIR studies in the present work give confirmative support to the latter “nucleophilic attack mechanism”, as discussed below. First, the formation of surface peroxo species, TiOOH and TiOOTi, as reaction intermediates (Figures 2 and 3), strongly supports the “nucleophilic attack mechanism”, as understood from the above arguments.

Second, the experiment of Figure 6 shows that the exposure of TiO₂ to H₂O₂ leads to a clear appearance of the 877-cm⁻¹ band assigned to free (physically adsorbed) H₂O₂, indicating that this band should be observed if H₂O₂ was produced at the TiO₂ surface. Thus, no appearance of this band in Figure 2 indicates that H₂O₂ (or •OH radicals as a precursor of it) was not produced as an intermediate of the oxygen photoevolution reaction. One might point out a possibility that H₂O₂, even if it was produced, would react with Fe²⁺, formed by the reduction of Fe³⁺, and disappear (Fenton reaction). We cannot exclude this possibility, but no appearance of the 877-cm⁻¹ band in the spectrum for Pt-loaded TiO₂ in an acidic solution with no Fe³⁺ [spectrum (b) in Figure 3] indicates that this possibility is not important. Furthermore, under the assumptions that the “surface-OH oxidation mechanism” is the correct mechanism and that all produced H₂O₂ molecules react with Fe²⁺ and disappear, we can explain no appearance of the 877-cm⁻¹ band but we cannot explain the production of surface peroxo species (TiOOH and TiOOTi) themselves. (The direct formation of TiOOTi via coupling of two adjacent [Ti •OH]_s⁺ radicals is impossible because of a long distance between the two radicals or the two Ti atoms.) In harmony with the above argument, Fujishima et

- (81) Yamada, H.; Hurst, J. K. *J. Am. Chem. Soc.* **2000**, *122*, 5303.
 (82) Root, D. E.; Mahroof-Tahir, M.; Karlin, K. D.; Solomon, E. I. *Inorg. Chem.* **1998**, *37*, 4838.
 (83) Jones, R.; Summerville, D. A.; Basols, F. *Chem. Rev.* **1979**, *79*, 2.
 (84) Nakamoto, K.; Nonaka, Y.; Ishiguro, T.; Urban, M. W.; Suzuki, M.; Kozuka, M.; Nishida, Y.; Kida, S. *J. Am. Chem. Soc.* **1982**, *104*, 3386.
 (85) Nakamoto, K. *Infrared and Raman Spectra of Inorganic and Coordination Compounds*; John Wiley & Sons: New York, 1986.
 (86) Gutsev, G. L.; Rao, B. K.; Jena, P. *J. Phys. Chem. A* **2000**, *104*, 11961.
 (87) Muller, J.; Schwarz, G. *Inorg. Chem.* **1970**, *9*, 2381.
 (88) Mikszal, R.; Valentine, J. S. *Inorg. Chem.* **1984**, *23*, 3548.
 (89) Kristine, F. J.; Shepherd, R. E.; Siddiqui, S. *Inorg. Chem.* **1981**, *20*, 2571.

Scheme 1. Reaction Scheme for the Oxygen Photoevolution Reaction on TiO₂ (Rutile) in Contact with an Aqueous Solution of pH of 1 to about 12



al.⁹⁰ reported very recently that H₂O₂ formation was not detected on UV-irradiated TiO₂ powder (P25) in the presence of Ag⁺ as an electron acceptor.

Third, the “nucleophilic attack mechanism” is strongly supported by the isotope-labeling experiments (Figure 5). We have to note first that the formation of ¹⁸O-containing surface species, such as Ti-¹⁶O-¹⁸OH, Ti-¹⁸O-¹⁶OH, Ti-¹⁸O-¹⁸OH, and Ti-¹⁸O-¹⁸O-Ti, clearly shows that surface TiOOH and TiOOTi, detected spectroscopically, are really formed by the water photooxidation reaction. The more important point is the formation of surface species containing both ¹⁶O and ¹⁸O such as Ti-¹⁶O-¹⁸OH and Ti-¹⁸O-¹⁶OH, which can be explained only by the “nucleophilic attack mechanism” for the following reasons. It is reported⁹¹ by using H₂¹⁸O that oxygen exchange between surface hydroxyl groups of TiO₂ and water in contact with it occurs quantitatively and rapidly in the dark at room temperature, whereas that between lattice oxygen and contacting water hardly occurs under the same conditions. This implies that, for TiO₂ in contact with H₂¹⁸O, all surface hydroxyl groups are substituted by ¹⁸OH. Thus, the incorporation of ¹⁶O into TiOOH unambiguously demonstrates that the water photooxidation is initiated by a nucleophilic attack of H₂¹⁸O to lattice oxygen (Ti-¹⁶O-Ti). If the water photooxidation proceeded via the “surface-OH oxidation mechanism”, only Ti-¹⁸O-¹⁸OH could be formed.

The “nucleophilic attack mechanism” is further supported by PL measurements. We mentioned in the preceding section that the PL spectra in acidic and alkaline solutions are identical to each other in spectral position and shape (Figure 8), indicating that the PL-emitting species is free from an acid–base equilibrium (i.e. it causes neither protonation nor deprotonation) in the pH range from 1 to 12. This result is in harmony with “nucleophilic attack mechanism” because, in this mechanism, the PL band is arising from the surface-trapped holes at the bottom of atomic grooves at the (100) face⁵¹ (Figure 9). On the other hand, this result cannot be explained by the “surface-OH oxidation mechanism”, for, in this mechanism, surface •OH radicals or related species have to be a possible PL-emitting species. Actually, Salvador et al.⁹² claimed long ago that the PL band was arising from adsorbed H₂O₂ or •OH radicals. However, such species as H₂O₂ and •OH cause deprotonation reaction in the pH range from 1 to 12, since pK_a of •OH is reported to be 11.5⁹³ and that of H₂O₂

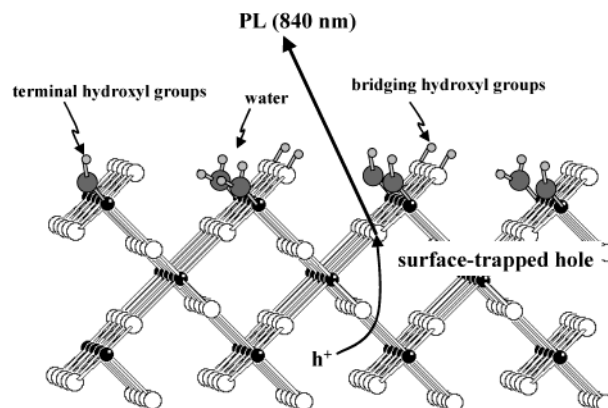


Figure 9. Schematic surface-lattice model for the (100) face of TiO₂ (rutile) in contact with an aqueous electrolyte, together with a photoluminescent process arising from a recombination of a surface-trapped hole at an atomic groove and an electron in the conduction band.

11.8.⁹⁴ The deprotonation reaction should largely change the electronic energy level for a luminescent species (•OH or H₂O₂), thus causing a large spectral shift in the PL band, contrary to the experimental result.

Finally, it is interesting to note that UPS studies have shown⁶⁴ that the top of the O-2p levels for surface hydroxyl groups (Ti-OH) at the rutile TiO₂ (100) face is about 1.8 eV below the top of the valence band, E_v^s , at the surface. This implies that surface hydroxyl groups cannot be oxidized by photogenerated holes in the valence band. Although the above energy is obtained under vacuum (i.e. at the TiO₂/vacuum interface), the same conclusion holds even for the TiO₂/water interface. A difference is that a cation formed by photoelectron ejection at the TiO₂ surface is stabilized at the TiO₂/water interface additionally by electronic polarization of water. A simple calculation of the electronic polarization energy ΔG_{el} of water for surface Ti-OH by use of the Born equation, $\Delta G_{el} = (e^2/8\pi\epsilon_0 r)(1 - 1/n^2)$, where r is the van der Waals radius for OH group of Ti-OH and n is the refractive index of water, leads to a value of $\Delta G_{el} = 2.1$ eV for $r = 0.15$ nm. For a surface species such as Ti-OH, only one-half of this ΔG_{el} (namely 1.1 eV) contributes because water occupies only a half space at the TiO₂/water interface. We can thus conclude that the top of the O-2p levels for Ti-OH at the TiO₂/water interface is about $(1.8 - 1.1) = 0.7$ eV below the E_v^s , and thus Ti-OH cannot be oxidized by valence-band holes.

In conclusion, we can propose a reaction scheme of Scheme 1 as the most plausible molecular mechanism for the oxygen photoevolution reaction at the TiO₂ (rutile) surface in contact

(90) Cai, R.; Kubota, Y.; Fujishima, A. *J. Catal.* **2003**, *219*, 214.

(91) Sato, S. *J. Phys. Chem.* **1987**, *91*, 2895.

(92) Salvador, P.; Gutiérrez, C. *J. Phys. Chem.* **1984**, *16*, 3698.

(93) Poskrebyshev, G. A.; Neta, P.; Huie, R. E. *J. Phys. Chem. A* **2002**, *106*, 11488.

(94) Weast, R. C. *Handbook of Chemistry and Physics*; CRC Press: Boca Raton, 1993.

with aqueous solutions of pH less than about 12. Of various intermediates, surface peroxo species, TiOOTi and TiOOH, are directly detected by in situ FTIR experiments. Scheme 1 is supported by isotope-labeling experiments and PL measurements. It is to be noted also that the surface species TiOOTi and TiOOH can really be regarded as intermediates of the oxygen photoevolution reaction on TiO₂, because it is reported⁹⁵

that stoichiometric oxygen evolution and Fe³⁺ reduction proceed with a high quantum efficiency of 17% under UV irradiation of a TiO₂ (rutile)–8 mM Fe³⁺ system.

JA0388764

(95) Fujihara, K.; Ohno, T.; Matsumura, M. *J. Chem. Soc., Faraday Trans.* **1998**, *94*, 3705.